Journal of Bioenergetics and Biomembranes, Vol. 34, No. 6, December 2002 (© 2002)

Purification and Characterization of the Complex I From the Respiratory Chain of *Rhodothermus marinus*

Andreia S. Fernandes,[1] Manuela M. Pereira,[1,2] and Miguel Teixeira[1]

Received August 8, 2002; accepted October 4, 2002

The rotenone sensitive NADH:menaquinone oxidoreductase (NDH-I or complex I) from the thermohalophilic bacterium *Rhodothermus marinus* has been purified and characterized. Three of its subunits react with antibodies against 78, 51, and 21.3c kDa subunits of *Neurospora crassa* complex I. The optimum conditions for NADH dehydrogenase activity are 50°C and pH 8.1, and the enzyme presents a K_M of 9 μM for NADH. The enzyme also displays NADH:quinone oxidoreductase activity with two menaquinone analogs, 1,4-naphtoquinone (NQ) and 2,3-dimethyl-1,4-naphtoquinone (DMN), being the last one rotenone sensitive, indicating the complex integrity as purified. When incorporated in liposomes, a stimulation of the NADH:DMN oxidoreductase activity is observed by dissipation of the membrane potential, upon addition of CCCP. The purified enzyme contains 13.5 ± 3.5 iron atoms and ~3.7 menaquinone per FMN. At least five iron–sulfur centers are observed by EPR spectroscopy: two $[2Fe–2S]^{2+/1+}$ and three $[4Fe–4S]^{2+/1+}$ centers. By fluorescence spectroscopy a still unidentified chromophore was detected in *R. marinus* complex I.

KEY WORDS: Complex I; NADH dehydrogenase; *Rhodothermus marinus*; menaquinone.

INTRODUCTION

The complex I of aerobic respiratory chains is NADH:quinone oxidoreductase (EC 1.6.99.3), also called NADH dehydrogenase, which catalyses the reduction of quinone by NADH, coupling electron transfer to proton translocation, with a stoichiometry of $\sim 4H^+/2e^-$. This reaction is inhibited by rotenone and piericidin A. Complex I is the least understood complex among the electron transfer chain components, which is due to its large multisubunit composition. The mitochondrial complex of higher eukaryotes comprises 43 different subunits, with a total molecular mass around 1 million Da, assuming that only one copy of each subunit is present in the complex (e.g., Finel, 1998; Friedrich *et al*., 1995; Ohnishi, 1998; Ohnishi *et al*., 1998; Rasmussin *et al*., 1998; Videira, 1998; Weiss *et al*., 1991).

Complex I has at least three different types of prosthetic groups: flavin (FMN), iron–sulfur clusters, and possibly three distinct protein-bound species of quinones. The presence of 1 or 2 mol of FMN per mol of enzyme is still under debate (Albracht *et al*., 1997; Albracht and Hedderich, 2000; Ohnishi, 1998), and the average reduction potential of FMN is ~−340 mV (Dutton *et al*., 1998). Regarding the iron–sulfur centers, their number and types is also an open question, although it is agreed the presence of two $[2Fe–2S]^{2+/1+}$ clusters (N1a and N1b), and four $[4Fe–4S]^{2+/1+}$ clusters (N2, N3, N4, and N5), detectable by EPR spectroscopy. Clusters N1a and N2 have reduction potentials of ~−370 mV and ~−150 mV, respectively, while N1b, N3, N4, and N5 form an isopotential group with reduction potentials around −250 mV (e.g., Friedrich *et al*., 1995; Ohnishi, 1998; Weiss *et al*., 1991).

A gross L-shape structure of the complex was obtained from image reconstruction pictures of

Key to abbreviations: CCCP, carbonyl cyanide *m*-chlorophenylhydrazon; DM, *n*-dodecyl-β-D-maltoside; DMN, 2,3-dimethyl-1,4-naphtoquinone; NADH, reduced nicotinamide adenine dinucleotide; dNADH, deaminoNADH; NDH, NADH dehydrogenase; NQ, 1,4-naphtoquinone; PMSF, phenylmethylsulfonyl fluoride; *R., Rhodothermus*; TCA, trichloroacetic acid; TFA, trifluoroacetic acid.

[1]Instituto de Tecnologia Química e Biológica, Universidade Nova de Lisboa, Rua da Quinta Grande 6, 2780-156 Oeiras, Portugal.

[2]To whom correspondence should be addressed; e-mail: mpereira@itqb.unl.pt.

0145-479X/02/1200-0413/0 © 2002 Plenum Publishing Corporation

electron microscopic patterns of two-dimensional crystals (Hofhaus *et al.*, 1991). One of the L arms is embedded in the membrane while the other is perpendicular to it. The arm facing the mitochondrial matrix or the bacterial cytoplasm is composed of several subunits comprising the flavo-containing one and most subunits containing the iron–sulfur centers. Cluster N2 seems to be the exception, being possibly situated in the intersection with the membrane (Ohnishi, 1998).

The known bacterial complexes I, called NDH-1, are composed of 13–14 different subunits and present the same properties as the mitochondrial one, i.e., non-covalently-bound FMN, multiple iron–sulfur clusters, and sensitivity to rotenone and piericidin A (Dupuis *et al.*, 1998; Friedrich, 1998; Yagi, 1993; Yagi *et al.*, 1998). In fact, bacterial NDH-1 is the minimal catalytic form of complex I: the seven most hydrophobic bacterial subunits correspond to mitochondrially encoded subunits and the other six or seven bacterial subunits correspond to homologous nuclear encoded subunits of the mitochondrial complex. This type of NADH dehydrogenase has only been observed in Proteobacteria, in *Thermus thermophilus* and *Aquifex aeolicus*.

Rhodothermus (R.) marinus is a thermohalophilic and strict aerobic bacterium. It has an unusual membrane-bound respiratory chain, containing a new complex III (a cytochrome *bc* complex; Pereira *et al.*, 1999a), and a HiPIP (Pereira *et al.*, 1994, 1999b) as an electron carrier between this complex and the caa_3 oxidase, which has a different intraprotein proton pathway (Pereira *et al.*, 1999c, 2000; Santana *et al.*, 2001). Its complex II constitutes an example of a well-characterized succinate:menaquinone oxidoreductase (Fernandes *et al.*, 2001). *R. marinus* possesses also a complex I (Pereira *et al.*, 1999b), whose purification, biochemical and spectroscopic characterization is reported here.

METHODS

Protein Purification

Bacterial growth, membrane preparation, and solubilisation were done as described in Pereira *et al.* (1999a). All chromatographic steps were performed on Pharmacia HiLoad or LKB-HPLC systems, at 4°C. The detergent solubilised membrane fraction was applied to a Q-Sepharose column, using as buffer 20 mM Tris-HCl (pH 7), 0.05% DM, and was eluted in a linear gradient of 0–50% 1 M NaCl. The fraction containing NADH dehydrogenase activity was then applied to a Chelating Sepharose Fast Flow column saturated with Ni^{2+} and equilibrated with 20 mM Tris-HCl (pH 7), 0.5 M NaCl, 0.1% DM. Two linear gradients of 0–10% and 10–100% 125 mM imidazole were applied. The NDH was eluted in the first gradient, being then applied to a gel filtration S200 column, eluted with 20 mM Tris-HCl (pH 7), 0.1% DM, 150 mM NaCl. All buffers included 1mM PMSF and 1mM EDTA, with the exception of the Chelating Sepharose column. After all purification steps the visible spectra were monitored and NADH dehydrogenase activity assays were performed.

Iron Content Determination

Iron content was determined by Atomic Absorption at Laboratório de Análises, Instituto Superior Técnico.

Flavin Extraction, HPLC Analysis, and Content Determination

Flavin was extracted according to Susín *et al.* (1993). Flavin composition was analysed on a System Gold, Beckman chromatograph with a Nova-pak C18 (3.9 × 150 mm, Waters) reverse phase HPLC column with two linear gradients of 0–15% and 15–100% methanol in ammonium acetate. Commercial FMN and FAD were used as standards. Flavin content was determined in purified enzyme by fluorescence spectroscopy (see below), using free FMN as standard.

Menaquinone Extraction, Purification, HPLC Analysis, and Content Determination

Menaquinone was extracted from the membranes according to Lemma *et al.* (1990) and further purified in a silica gel column eluted with a gradient of 1–9% diethylether in *n*-pentane. Menaquinone was extracted from purified NDH with 2-butanol. This extract was analyzed on a System Gold, Beckman chromatograph with a Nova-Pak C18 (3.9 × 150 mm, Waters) reverse phase HPLC column with a gradient of 30–100% methanol in 0.05% TFA. Menaquinone purified from the membranes was used as standard. Menaquinone content was determined by the absorption at 325 nm ($\varepsilon = 3080\ M^{-1}\ cm^{-1}$) and by measuring the areas of the peaks in the HPLC chromatogram.

Electrophoresis

Molecular masses were determined by tricine SDS-PAGE as described in Schägger and von Jagow (1987) with 10%T/3%C performed in a Laemmli discontinuous buffer system at 4°C. The sample buffer contained 8 M urea and

10% SDS to ensure an efficient exchange of detergent and denaturation, and the DM content of the sample was decreased to one-half before the incubation with the loading buffer. The gel was stained with Silver Staining (Blum *et al.*, 1987).

Amino Acid Sequencing

For peptide sequencing, the enzyme subunits were separated by the electrophoretic procedure described above and transferred to a polyvinylidene difluoride (PVDF) membrane. Each transblotted sample was submitted to N-terminal protein sequence analysis by automated Edman degradation (Edman and Begg, 1967), using an Applied Biosystem model 470A sequencer.

Immunoblotting

The enzyme subunits separated by the electrophoretic procedure described above were transferred to a Nitrocellulose membrane and incubated with antibodies against subunits 78, 51, 49, 30.4, 24, 21.3c, and 19.3 kDa of *Neurospora crassa* (the antibodies used were a kind gift of Prof Arnaldo Videira from IBMC, Portugal). Anti-rabbit IgG was used as second antibody and the detection was performed with 3-bromo-4-chloro-3-indolylphosphate and nitro blue tetrazolium.

Spectroscopic Techniques

UV–Visible absorption spectra were obtained on a Shimadzu UV-1603 spectrophotometer, at room temperature. EPR spectra were obtained as in Pereira *et al.* (1999a). The spectra obtained were theoretically simulated using the Aasa and Vänngard approach (Aasa and Vänngard, 1975). Fluorescence spectra were obtained on a Spex 212 spectrophotometer with L configuration and double monochromators.

Reconstitution of Purified Complex I Into Liposomes

80 mg/mL of asolectin and ∼0.5 mg/mL of 1,4-naphthoquinone were sonicated in 50 mM HEPES buffer (pH 7.5), 1.6% *n*-octyl-β-D-glucopyranoside. Approximately 77 pmol of *R. marinus* complex I (protein content was determined considering 1 FMN per complex) were incubated at 4°C with the sonicated solution under agitation for 15 min. After 30 and 90 min of incubation, 100 mg of Bio-Beads were added; after 150 min more 500 mg were added. To confirm that the liposomes were not leaky, it was performed a spectrophotometric assay following the membrane potential indicator oxonol at 628–587 nm, upon addition of 2 μM valinomycin to the liposomes with the reconstituted complex, in 50 mM HEPES buffer (pH 7.5), 50 mM K_2SO_4, and in the presence of 2 μM oxonol.

Catalytic Activity Assays

Activity assays were performed on a Shimadzu UV-1603 or on an Olis DW2 spectrophotometers. NADH oxidase activity in *R. marinus* membranes was followed at 38°C by measuring oxygen consumption polarographically with a Clark-type oxygen electrode, YSI Model 5300, Yellow Springs. The reaction mixture contained 20 mM Tris-HCl (pH 7.6) buffer and sample, and the reaction was started by the addition of NADH.

NADH dehydrogenase activity of complex I was monitored by following the $K_3[Fe(CN)_6]$ reduction at 420 nm ($\varepsilon = 1020\ M^{-1}\ cm^{-1}$). The reaction mixture contained 20 mM Tris-HCl (pH 7.6), 0.1% DM buffer, 1 mM $K_3[Fe(CN)_6]$, and 0.2 mM NADH. The reaction was started by the addition of sample.

NADH or dNADH:quinone oxidoreductase activities of complex I were monitored anaerobically under argon at 55°C following the oxidation of NADH or dNADH at 340 nm ($\varepsilon = 6220\ M^{-1}\ cm^{-1}$) when the acceptor quinone was 1,4-naphtoquinone (NQ) or at 330 nm ($\varepsilon = 5930\ M^{-1}\ cm^{-1}$) when the acceptor was 2,3-dimethyl-1,4-naphtoquinone (DMN). The reaction mixture contained 100 mM potassium phosphate buffer (pH 7.5), 0.1% DM, 0.2 mM quinone, and 0.1 mM NADH. The reaction was started by the addition of sample or quinone. For studies with rotenone, the sample was incubated for 5 min with rotenone in concentrations between 0 and 0.2 mM prior to the addition of NADH and quinone and for the studies with lipids asolectin was used. The same procedure was followed with liposome reconstituted complex I, but 50 mM HEPES buffer (pH 7.5), 50 mM K_2SO_4 was used instead.

Turnover numbers and specific activities were calculated by the FMN content considering 1 mol of FMN per mol of complex. The specific activities calculations assumed the mass 800 kDa for the complex.

RESULTS AND DISCUSSION

Evidence for the Existence of a Complex I in *R. marinus*

R. marinus membranes show consumption of oxygen with a rate of 0.049 nmol O_2 mg^{-1} s^{-1} at 38°C

upon addition of NADH, implying the presence of a NADH:quinone oxidoreductase. Upon the addition of the specific inhibitor of the complex I rotenone in a concentration of 78 μM, the observed rate of oxygen consumption decreases ca. 70%. However, if the membranes are previously incubated with the same amount of rotenone prior to the addition of NADH, the rate of oxygen consumption becomes negligible.

NADH and dNADH oxidation activities were followed in the membranes of *R. marinus*, using $K_3[Fe(CN)_6]$ and 1,4-naphthoquinone (NQ) as electron acceptors. The oxidation of NADH was also followed using 2,3-dimethyl-1,4-naphtoquinone (DMN) and decylubiquinone (DBQ). The specific activities obtained were the same for NADH/dNADH:$K_3[Fe(CN)_6]$ oxidoreductase (2.75 nmol NADH/dNADH mg^{-1} s^{-1}), and NADH/dNADH:NQ oxidoreductase activities (5.46 nmol NADH/dNADH mg^{-1} s^{-1}). The specific activity for NADH:DMN oxidoreductase was 1.48 nmol NADH mg^{-1} s^{-1} and the NADH:DBQ oxidoreductase activity was negligible. EPR studies in *R. marinus* membranes had shown previously (Pereira *et al.*, 1999b) that the addition of NADH led to the development of resonances typical of reduced iron–sulfur centers of the $[2Fe–2S]^{2+/1+}$ and $[4Fe–4S]^{2+/1+}$ types. These observations provide evidence for the presence of a complex I in *R. marinus* respiratory chain.

Biochemical Characterization

The elution profiles of the chromatographic steps performed for the purification of *R. marinus* NDH-I are shown in Fig. 1. *R. marinus* NDH-I shows ~14 subunits on a SDS-PAGE, with apparent molecular masses ranging from ~100 to 19 kDa (Fig. 2(A)). Altogether, the apparent masses of the subunits sum up to 800 kDa. No similarity was found between the N-terminal sequences obtained and those on the public databases, but this is not surprising since the similarity of the N-termina among each complex I subunit is negligible.

To further identify the subunits of *R. marinus* complex I, immunoblotting with antibodies against subunits of the *Neurospora crassa* complex I was performed. A subunit with an apparent molecular mass of 45 kDa strongly reacted with the antibody against the 51 kDa subunit (NQO1 from *Paracoccus denitrificans*). Two other weaker reactions could be observed between the antibodies against subunits 78 and 21.3c kDa (respectively NQO3 and NQO9 from *Paracoccus denitrificans*), and *R. marinus* NDH subunits of apparent masses 66 and 25 kDa, respectively (Fig. 2(B)).

Flavin extraction and HPLC analysis revealed the presence of non-covalently-bound FMN in the purified

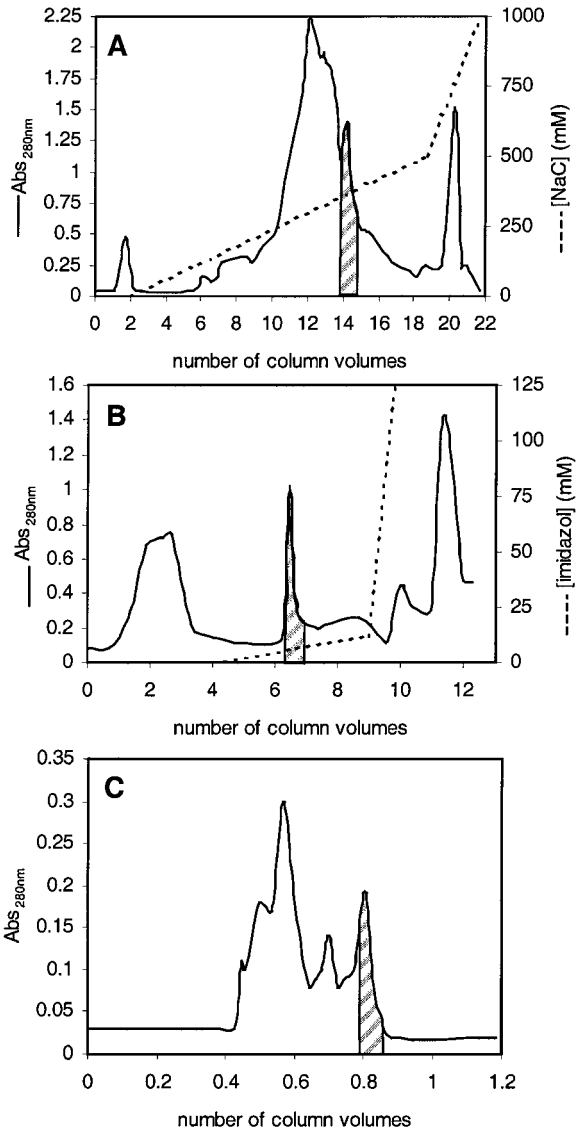

Fig. 1. Purification of *R. marinus* complex I. (A) Elution profile from Q-Sepharose loaded with *R. marinus* solubilized membranes. (B) Elution profile from Chelating Sepharose loaded with the NDH containing fraction from Q-Sepharose. (C) Elution profile from S200 loaded with the NDH containing fraction from Chelating Sepharose. The NDH containing fractions colected in each cromatografic step are marked with a striped pattern.

enzymatic complex. FMN was quantified by fluorescence spectroscopy (see below). The iron content was quantified by atomic absorption and a ratio of $13.5 + 3.5$ iron/flavin was obtained.

A quinone was also extracted from the purified complex, which by HPLC analysis gave a pattern identical to that of menaquinone extracted from *R. marinus* membranes. In both cases, three peaks were eluted. The third one exhibits an UV-Visible spectrum typical of

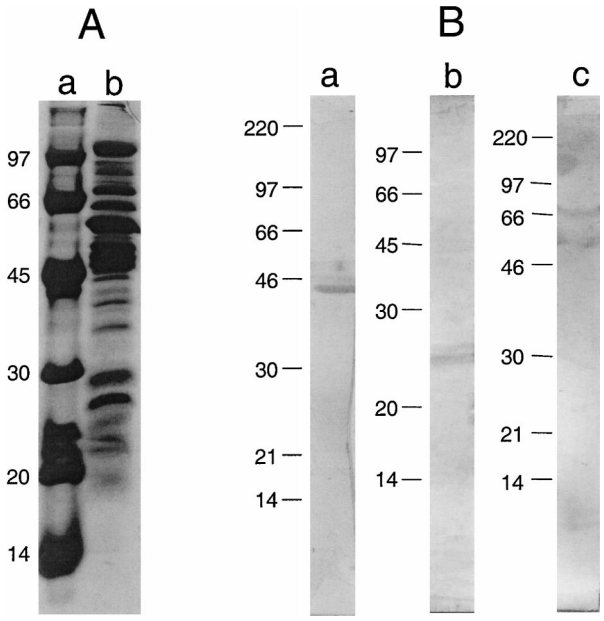

Fig. 2. (A) SDS-Polyacrilamide gel of purified *R. marinus* NADH desidrogenase (b) and molecular mass standards in kDa (a). (B) Incubation of *R. marinus* complex I subunits with antibodies against *Neurospora crassa* complex I subunits 51 kDa (a), 21.3c kDa (b), and 78 kDa (c). Molecular mass standards positions are indicated on the left of each marker.

menaquinone, with a maximum of absorption at 327 nm (Fig. 3(A)), and when excited at this wavelength, emission with a maximum at 426 nm is observed (Fig. 3(B)). The same behavior is obtained with commercial menaquinone-4, used here as a standard. The ratio of menaquinone/flavin obtained was 3.7, after quantification of the product eluted in the third peak. This result is consistent with the three distinct quinone species observed in complex I (Yano and Ohnishi, 2001), if 1 FMN per molecule of enzyme is considered.

It has been reported that menaquinone degrades by photooxidation (Brito *et al.*, 1995). In order to check whether this was the origin of the other two peaks eluted in the HPLC analysis, the peak containing menaquinone (the third one) was reapplied in the HPLC column and subjected to the same elution program. The chromatogram obtained showed the presence of two peaks coincident with the first chromatogram: one corresponding to the menaquinone itself and the other having the same retention time as the peak first eluted in the first chromatography. It was not observed any peak eluting with the same retention time as the second peak in the first chromatography. This indicated that probably the compound eluted in the first peak results from some degradation of menaquinone and the second peak eluting corresponds to a different compound that copurifies with menaquinone, probably a lipid, as suggested by its UV-Visible absorption spectrum (not shown).

Functional Analysis

The purified enzyme presents a turnover number of 1905 s^{-1} (2.38 μmol NADH s^{-1} mg^{-1}) for NADH dehydrogenase activity (using $K_3[Fe(CN)_6]$ as the electron

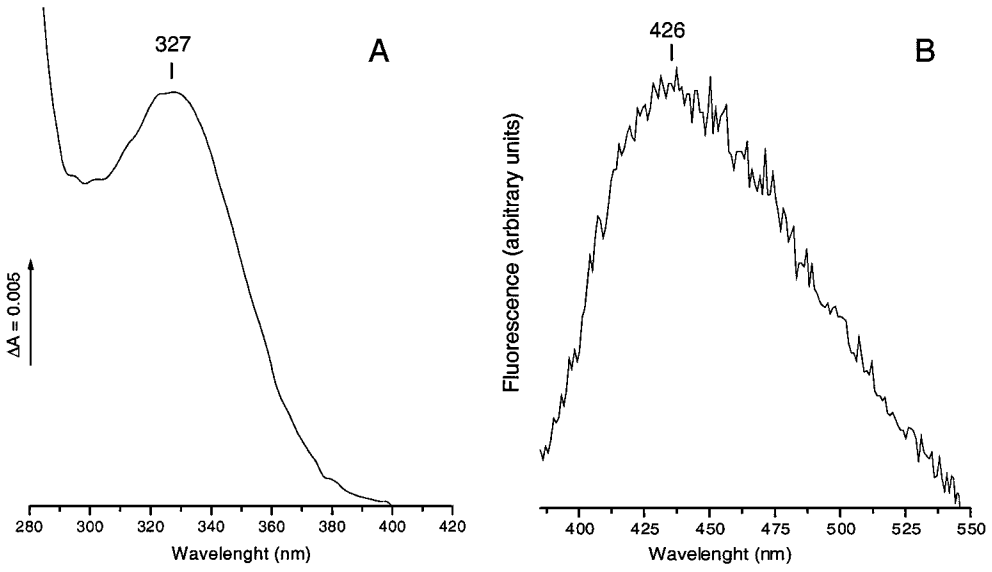

Fig. 3. Spectroscopic characterization of the menaquinone eluted in the third peak of the HPLC (see text): absorption UV–Visible spectrum (A) and fluorescence emission spectrum with excitation at 327 nm (B).

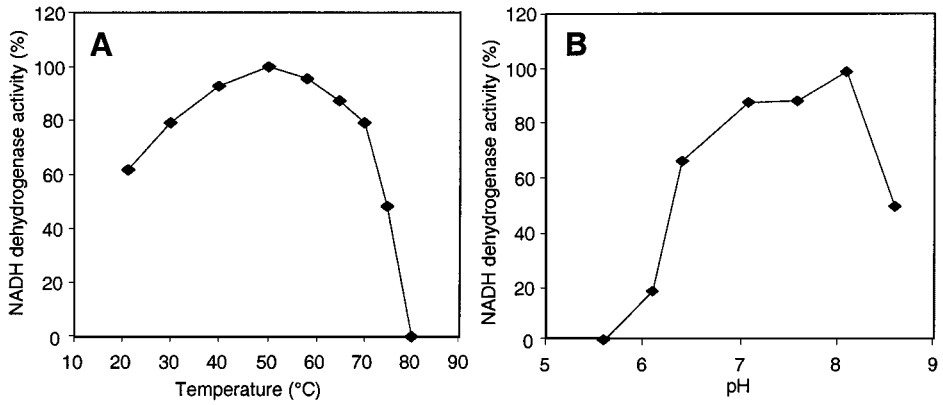

Fig. 4. (A) Temperature (at pH 7.5) and (B) pH (at 65°C) profiles of NADH:$K_3[Fe(CN)_6]$ oxidoreductase activity of *R. marinus* NADH dehydrogenase.

acceptor) at 55°C, if one mol of FMN per mol of protein is considered. The optimum temperature for NADH dehydrogenase activity is 50°C (Fig. 4(A)), which is lower than the optimum growth temperature of *R. marinus* (65°C). At 70°C, 80% of the maximum of activity is still retained. The optimum pH for this activity is 8.1 (Fig. 4(B)). The K_M for NADH was determined to be 9 μM at 65°C, comparable with that found for the bovine mitochondrial complex, 3.5 μM (Okun *et al*., 1999).

The integrity of the purified complex I from *R. marinus* was inspected monitoring NADH:quinone oxidoreductase activity in the purified complex. Two menaquinone analogues were tried: 1,4-naphtoquinone (NQ) and 2,3-dimethyl-1,4-naphtoquinone (DMN). A turnover number of 2561 s^{-1} (3.2 μmol NADH s^{-1} mg^{-1}) at 55°C was obtained when NQ was used, and this activity was insensitive to rotenone. In the assay with DMN, a turnover number of 479 s^{-1} (0.60 μmol NADH s^{-1} mg^{-1}) was observed (Fig. 5(A)). These high activities may reflect the fact that DMN and NQ are close analogs of menaquinone, the main quinone present in *R. marinus*. NADH:DMN oxidoreductase activity was titrated with rotenone, the typical inhibitor of complex I, and it was observed a decrease of 40% for concentrations of rotenone above 50 μM (Fig. 5(B)). The NADH:DMN oxidoreductase activities with and without rotenone were also performed in the presence of lipids, and the same turnover numbers and inhibition extension as in the absence of lipids were observed. The fact that *R. marinus* NDH-I is inhibited by rotenone implies that the electron transfer pathway in the protein complex from the flavin to the quinone binding site is intact. That indicates that the purification of the complex I from *R. marinus* has been achieved without the loss of integrity of the complex, which is very difficult with the bacterial complex I, since in most cases the peripheral arm disagregates from the

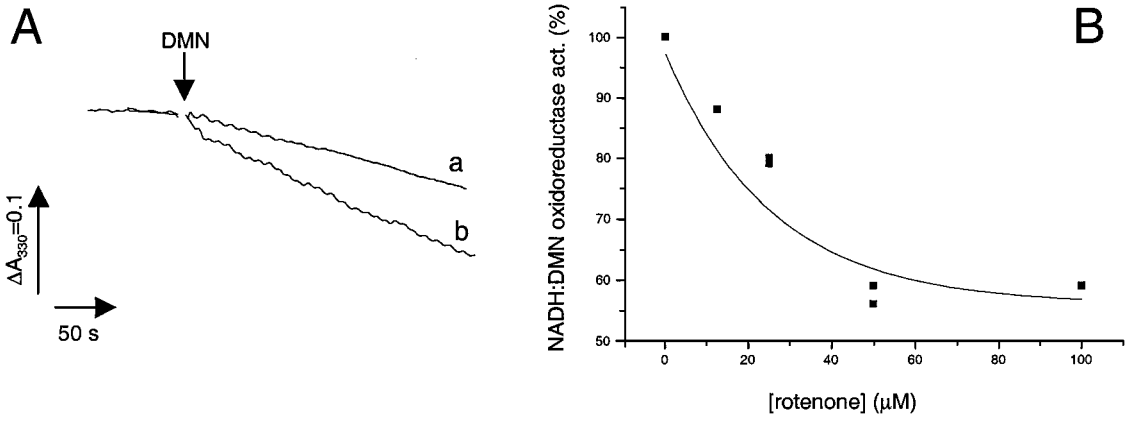

Fig. 5. (A) NADH:DMN oxidoreductase activity of purified complex I from *R. marinus*. The enzyme was incubated for 5 min with 0.1 mM NADH and 1% dimethylsulphoxide, in the absence (a) and presence (b) of 50 μM rotenone. The reaction was started with the addition of 0.2 mM DMN. (B) Titration curve of the inhibitor effect of rotenone in NADH:DMN oxidoreductase activity.

membrane arm. In fact, the enzyme was purified with iron–sulfur centers and FMN, present in the peripheral arm, and also menaquinone, believed to be present in the membrane arm.

The purified enzyme is also able to catalyse the oxidation of dNADH, with the same rate as the oxidation of NADH when the acceptor is NQ and with 79% of the rate when the acceptor is $K_3[Fe(CN)_6]$.

The liposome reconstituted complex shows the same catalytic properties as the solubilised complex: it displays NADH:$K_3[Fe(CN)_6]$ oxidoreductase activity (326 s^{-1}; 0.65 μmol NADH s^{-1} mg^{-1}) and the two NADH:quinone oxidoreductase activities tried [242 s^{-1} (0.30 μmol NADH s^{-1} mg^{-1}) for NQ and 25.6 s^{-1} (0.032 μmol NADH s^{-1} mg^{-1}) for DMN). These activities are lower than the activity of the purified complex since due to the liposome stability they were obtained at 30°C and not at 55°C, the optimal temperature for *R. marinus* NDH-I. On the other hand, the values were obtained considering that all the protein in solution was reconstituted, which most probably is not the case. The activity of NADH:DMN oxidoreductase is inhibited by rotenone in the same extent as in the purified protein. Moreover, this activity was stimulated up to 54% by dissipating the membrane electrochemical proton gradient with 20 μM of the uncoupler CCCP in the course of the reaction (Fig. 6), what is in accordance with a proton-translocating complex. When NQ was used instead of DMN, no stimulation was observed. This fact, together with the rotenone insensitive NADH:NQ oxidoreductase activity, suggests that NQ and DMN bind to different sites in the enzyme, being DMN (but not NQ) able to bind at the quinone binding site coupled with proton translocation.

Spectroscopic Characterization

The electronic absorption spectra of *R. marinus* NDH in the oxidised form is typical of proteins containing iron–sulfur centers and flavin as prosthetic groups (Fig. 7).

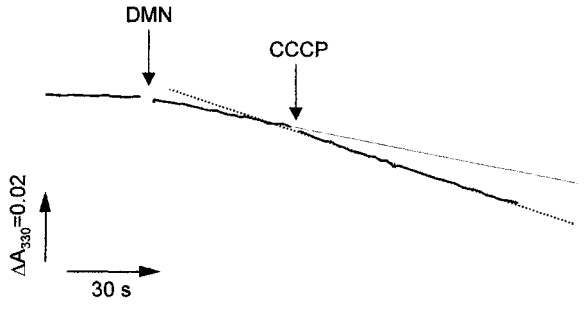

Fig. 6. Stimulation of NADH:DMN oxidoreductase activity of the liposome reconstituted complex I from *R. marinus* with the uncoupler CCCP (20 μM).

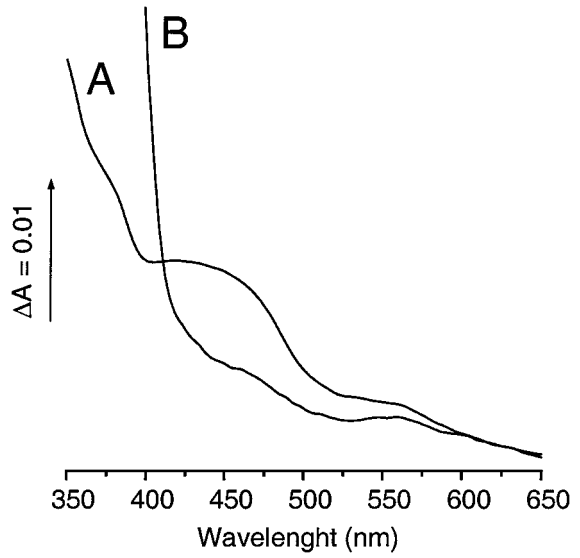

Fig. 7. Visible spectrum of *R. marinus* purified NDH in the oxidised (A) and NADH reduced (B) states.

Flavin content was determined by measuring the fluorescence intensity at 535 nm when exciting the intact purified protein at 445 nm (flavin maximum of absorption), and by comparison with a standard solution of FMN. The same result was obtained when flavin extracted from the purified NDH with TCA was used instead of intact enzyme, what means that all the flavin in the protein is excited and that no fluorescence quenching occurs when the flavin is embedded in the protein. By performing the excitation spectrum of NDH with emission at 535 nm, a pattern typical of flavin is obtained (Fig. 8(A)). A second fluorescent emission band with a maximum at 397 nm was observed, when exciting the intact purified protein at

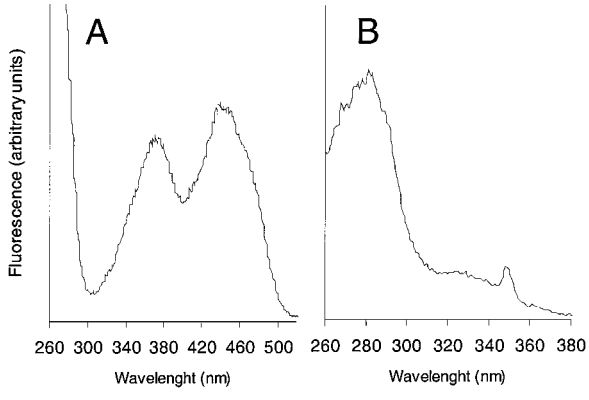

Fig. 8. Fluorescence spectra of *R. marinus* purified NDH. (A) Excitation spectrum with emission at 535 nm. (B) Excitation spectrum with emission at 397 nm.

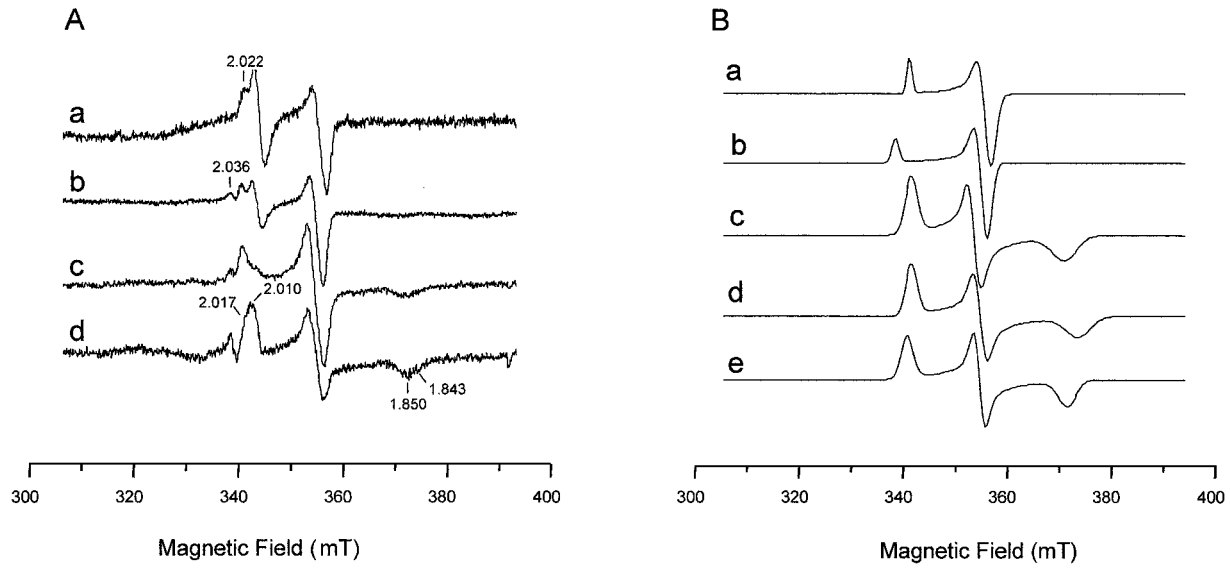

Fig. 9. (A) EPR spectra of *R. marinus* purified complex I reduced with NADH at different temperatures: (a) 43 K, (b) 34 K, (c) 10 K, (d) 4 K. Microwave power: 20 dB; microwave frequency: 9.64 GHz; modulation amplitude: 0.9 mT. (B) Different components present in (A) obtained by spectral deconvolution and simulation using the g values presented in Table I.

340 nm. By performing the corresponding excitation spectrum, a different chromophore was observed (Fig. 8(B)). Although one cannot rule out the hypothesis of a contamination, this spectrum was not observed in the buffer itself and is not due to the detergent DM, so it is attributed to an as yet unidentified chromophore.

A characterisation of the iron–sulfur centers in *R. marinus* NADH dehydrogenase by EPR spectroscopy was performed. Spectra of the purified complex reduced with excess of NADH were obtained at different temperatures and microwave powers. By carefully comparing the spectra obtained and by theoretical simulations, at least five distinct iron–sulfur centers could be assigned (Fig. 9 and Table I). An axial signal with g values of 2.022, 1.937, and 1.937 observed at 43 K was attributed to a reduced [2Fe–2S]$^{2+/1+}$ centre (Fig. 9, spectra Aa and Ba). The observed component with g value around 2.00 is due to a radical species. At 34 K (Fig. 9(A), spectrum b) two signals were observed, one corresponding to the [2Fe–2S]$^{2+/1+}$ center observed before and another attributed to a quasi-axial signal with g values of 2.036, 1.941, and 1.934 (Fig. 9(B), spectrum b). This signal was also attributed to a reduced [2Fe–2S]$^{2+/1+}$ center. From the spectra obtained at 10 K and at 4 K, three other set of resonances could be identified. The spectrum obtained at 4 K was simulated with two rhombic components with g values of 2.010, 1.941, and 1.850 (Fig. 9(B), spectrum c) and 2.017, 1.941, and 1.843 (Fig. 9(B), spectrum d). The deconvolution of the spectrum obtained at 10 K showed the presence of these two rhombic signals and the two axial signals identified before, and an additional rhombic signal with g values of 2.022, 1.941, and 1.854 (Fig. 9(B), spectrum e). Taking into account their relaxation properties the rhombic signals were attributed to three reduced [4Fe–4S]$^{2+/1+}$ centers.

Table I. Iron–Sulfur Centers Detected by EPR Spectroscopy in *R. marinus* Complex I Reduced With NADH

Spectra in Fig. 9(B)	Center type	g_{max}	g_{med}	g_{min}
(a)	[2Fe–2S]$^{2+/1+}$	2.022	1.937	1.937
(b)	[2Fe–2S]$^{2+/1+}$	2.036	1.941	1.934
(c)	[4Fe–4S]$^{2+/1+}$	2.010	1.941	1.850
(d)	[4Fe–4S]$^{2+/1+}$	2.017	1.941	1.843
(e)	[4Fe–4S]$^{2+/1+}$	2.022	1.941	1.854

The two [2Fe–2S]$^{2+/1+}$ and the three [4Fe–4S]$^{2+/1+}$ centers detected by EPR correlate well with the ratio of 13.5 ± 3.5 iron/flavin obtained, if one FMN per molecule of enzyme is considered. The three subunits identified by imunodetection (51, 78, and 21.3c kDa from *Neurospora crassa* or NQO1, 3 and 9 from *Paracoccus denitrificans*) allied with the two [2Fe–2S]$^{2+/1+}$ and the three [4Fe–4S]$^{2+/1+}$ centers show that all the subunits from the peripheral arm are most probably present in *R. marinus* purified NDH.

Because of their phylogenetical closeness to the mitochondrial respiratory chain, the best studied respiratory

chains are those from purple bacteria. Being a thermohalophilic bacterium belonging to the *Flexibacter–Cytophaga–Bacteroids* Group, *R. marinus* is an exemplar organism possessing different respiratory complexes (Pereira *et al.*, 1999a,b,c). Besides a succinate:quinone oxidoreductase (Fernandes *et al.*, 2001), *R. marinus* has a unique complex III (Pereira *et al.*, 1999a) and a caa_3 oxygen reductase with properties different from the reductases of purple bacteria (Pereira *et al.*, 1999c; Santana *et al.*, 2001). The study of its respiratory chain has now been further completed with the isolation and characterization of its NADH:quinone oxidoreductase, here reported. This complex is a typical complex I being its activity rotenone inhibited and sensitive to the membrane electrochemical proton potential. The isolation of the intact complex will allow its extensive characterization, including attempts to its crystallization.

ACKNOWLEDGMENTS

DMN was a kind gift of Prof Gottfried Unden from Institut für Mikrobiologie und Weinforschung, Germany. We thank the Photochemistry group from ITQB for technical assistance with fluorescence spectroscopy, Margarida Duarte from IBMC for assistance with the antibody technique, and Manuela Regalla for N-terminal determination. A. S. Fernandes and M. M. Pereira are recipients of grants from Praxis XXI program (BD/1163/00 and BPD/22054/99). This work was supported by Fundação para a Ciência e a Tecnologia (POCTI/BME/36560/99).

REFERENCES

Aasa, R., and Vänngard, V. T. (1975). *J. Magn. Res.* **19**, 308–315.
Albracht, S. P. J., and Hedderich, R. (2000). *FEBS Lett. 485*, 1–6.
Albracht, S. P. J., Mariette, A., and de Jong, Ph. (1997). *Biochim. Biophys. Acta* **1318**, 92–106.
Blum, H., Beier, H., and Gross, H. J. (1987). *Electrophoresis* **8**, 93–99.
Brito, F., DeMoss, J. A., and Dubourdieu, M. (1995). *J. Bacteriol.* **177**, 3728–3735.
Dupuis, A., Chevallet, M., Darrouzet, E., Duborjal, H., Lunardi, J., and Issartel, J. P. (1998). *Biochim. Biophys. Acta* **1364**, 147–165.
Dutton, P. L., Moser, C. C., Sled, V. D., Daldal, F., and Ohnishi, T. (1998). *Biochim. Biophys. Acta* **1364**, 254–257.
Edman, P., and Begg, G. (1967). *Eur. J. Biochem.* **1**, 80–90.
Fernandes, A. S., Pereira, M. M., and Teixeira, M. (2001). *J. Bioenerg. Biomembr.* **33**, 343–352.
Finel, M. (1998). *Biochim. Biophys. Acta* **1364**, 112–121.
Friedrich, T. (1998). *Biochim. Biophys. Acta* **1364**, 134–146.
Friedrich, T., Steinmuller, K., and Weiss, H. (1995). *FEBS Lett.* **367**, 107–111.
Hofhaus, G., Weiss, H., and Leonard, K. (1991). *J. Mol. Biol.* **221**, 1027–1043.
Lemma, E., Unden, G., and Kröger, A. (1990). *Arch. Microbiol.* **155**, 62–67.
Ohnishi, T. (1998). *Biochim. Biophys. Acta* **1364**, 186–206.
Ohnishi, T., Sled, V. D., Yano, T., Yagi, T., Burbaev, D. S., and Vinogradov, A. D. (1998). *Biochim. Biophys. Acta* **1365**, 301–308.
Okun, J. G., Lümmen, P., and Brandt, U. (1999). *J. Biol. Chem.* **274**, 2625–2630.
Pereira, M. M., Antunes, A. M., Nunes, O. C., Costa, M. S., and Teixeira, M. (1994). *FEBS Lett.* **352**, 327–330.
Pereira, M. M., Carita, J. N., and Teixeira, M. (1999a). *Biochemistry* **38**, 1268–1275.
Pereira, M. M., Carita, J. N., and Teixeira, M. (1999b). *Biochemistry* **38**, 1276–1283.
Pereira, M. M., Santana, M., Soares, C. M., Mendes, J., Carita, J. N., Fernandes, A. S., Saraste, M., Carrondo, M. A., and Teixeira, M. (1999c). *Biochim. Biophys. Acta* **1413**, 1–13.
Pereira, M. M., Verkhovskaya, M. L., Teixeira, M., and Verkhovsky, M. I. (2000). *Biochemistry* **39**, 6336–6340.
Rasmussin, A. G., Heiser, V., Zabaleta, E., Brennicke, A., and Grohmann, L. (1998). *Biochim. Biophys. Acta* **1364**, 101–111.
Santana, M., Pereira, M. M., Elias, N. P., Soares, C. M., and Teixeira, M. (2001). *J. Bacteriol.* **183**, 687–699.
Schägger, H., and von Jagow, G. (1987). *Anal. Biochem.* **166**, 368–379.
Susín, S., Abián, J., Sánchez-Baeza, F., Peleato, M. L., Abadía, A., Gelpí, E., and Abadía, J. (1993). *J. Biol. Chem.* **268**, 20958–20965.
Videira, A. (1998). *Biochim. Biophys. Acta* **1364**, 89–100.
Weiss, H., Friedrich, T., Hofhaus, G., and Preis, D. (1991). *Eur. J. Biochem.* **197**, 563–576.
Yagi, T. (1993). *Biochim. Biophys. Acta* **1141**, 1–17.
Yagi, T., Yano, T., Di Bernardo, S., and Matsuno-Yagi, A. (1998). *Biochim. Biophys. Acta* **1364**, 125–133.
Yano, T., and Ohnishi, T. (2001). *J. Bioenerg. Biomembr.* **33**, 213–222.